Small-Angle X-ray Scattering Investigations of Novel Superstructures in Combined Chiral Liquid Crystalline Polymers

H. Mensinger* and A. Biswas†

Max-Planck-Institut für Polymerforschung, Postfach 3148, D-6500 Mainz, Germany

H. Poths

Institut für Organische Chemie, Universität Mainz, Becher Weg 18-22, D-6500 Mainz, Germany

Received October 22, 1991; Revised Manuscript Received February 4, 1992

ABSTRACT: A series of combined liquid crystalline polymers consisting of achiral main-chain mesogens and chiral side-chain mesogens have been investigated using small-angle X-ray scattering (SAXS). The data from unoriented and oriented samples reveal the presence of novel superstructures corresponding to bilayered and trilayered structural repeats in the smectic phase. On the basis of the analysis of the temperature-dependent SAXS data and structure–property relationships in similar low molecular weight liquid crystals, antiferroelectric ordering and ferrielectric ordering have been proposed for the bilayered and trilayered superstructures, respectively. The influence of the chemical structures of the main-chain and side-chain mesogens on the smectic layer spacing and on the formation of the superstructure is discussed.

Introduction

Liquid crystalline polymers (LCPs) are a class of polymers which have been intensely investigated for more than a decade.[1-3] These polymers can be broadly classified under two categories, namely, main-chain LCPs, where the mesogenic groups are part of the chain backbone, and side-chain LCPs, where the mesogenic groups are attached to the chain backbone, usually via flexible spacers. In the recent past, a variety of LCPs with new architectures have been synthesized, varying in the manner in which mesogenic groups are incorporated into the polymer chain.[4,5] One such example is a combined LCP, where side chains, consisting of mesogenic groups with flexible spacers, are attached in between mesogenic groups with flexible spacers in the main chain, as shown schematically in Figure 1. The synthesis and characterization of a series of combined LCPs, using different combinations of main-chain and side-chain mesogens, have been reported in the literature.[6,7] These studies have indicated that combined LCPs of the type shown in Figure 1 have a strong tendency toward forming smectic mesophases, where the main-chain and side-chain mesogens align parallel to each other to form layers in a smectic phase.[7]

The classification of smectic mesophases, developed through the study of low molecular weight liquid crystals, is based primarily on the nature of the intermolecular interaction within each smectic layer.[8] In recent years, there has been a lot of interest in the study of superstructures arising as a result of density fluctuations between and across layers, particularly in highly polar liquid crystals, leading to the formation of polymorphic smectic-A or smectic-C mesophases.[9,10] Another area of intense investigation has been the study of chiral smectic liquid crystals, following the prediction by Meyer and coworkers[11] that a spontaneous net polarization develops along the layer in the chiral smectic-C phase. The resulting phenomenon of ferroelectricity has been demonstrated in a multitude of chiral smectic systems, many of which have found application in electrooptical devices with fast switching times.[12] Chiral smectic phases also exhibit superstructures which arise as a result of a helical twist

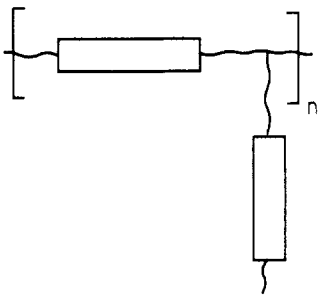

Figure 1. Molecular architecture in the combined liquid crystal polymer.

of the polarization vector with respect to the layer normal. The pitch of the helix is usually in the micron range,[12] corresponding to a few hundred layers (a typical layer is a few nanometers thick). Recent observations of local variations in the structural order between layers, leading to antiferroelectric and ferrielectric phases in chiral smectic liquid crystals, have increased interest in the study of superstructures and their interactions with external fields, both at the microscopic and macroscopic level.[13-15]

Polymeric liquid crystals also exhibit chiral phases.[16] Recently, it has been reported that the incorporation of side chains containing chiral groups in combined LCPs leads to the formation of chiral smectic phases.[17] A lot of research is being focused on the optimization of the structure and properties of chiral LCPs for applications not only in electrooptical devices but also in piezoelectric and nonlinear optical devices.[18-21] In this paper, we report on our investigations of a series of combined LCPs having chiral smectogens as side chains, using small-angle X-ray scattering (SAXS). Analysis of the data from unoriented and oriented samples reveals the presence of novel superstructures, which to our knowledge have not been observed in similar polymers before.

Experimental Section

The chemical structures of the combined LCPs under study are shown in Figure 2 and are numbered 1–7. The combined LCPs with chiral side-chain mesogens were prepared using a polymer-analogous esterification which allows the synthesis of both racemic and chiral polymers starting from the same precursor polymer.[22-24] As an example, the reaction scheme for the synthesis of the racemic LCP 5 is shown.

† Present address: Du Pont Experimental Station, P.O. Box 80356, Wilmington, DE 19880-0356.

0024-9297/92/2225-3156$03.00/0

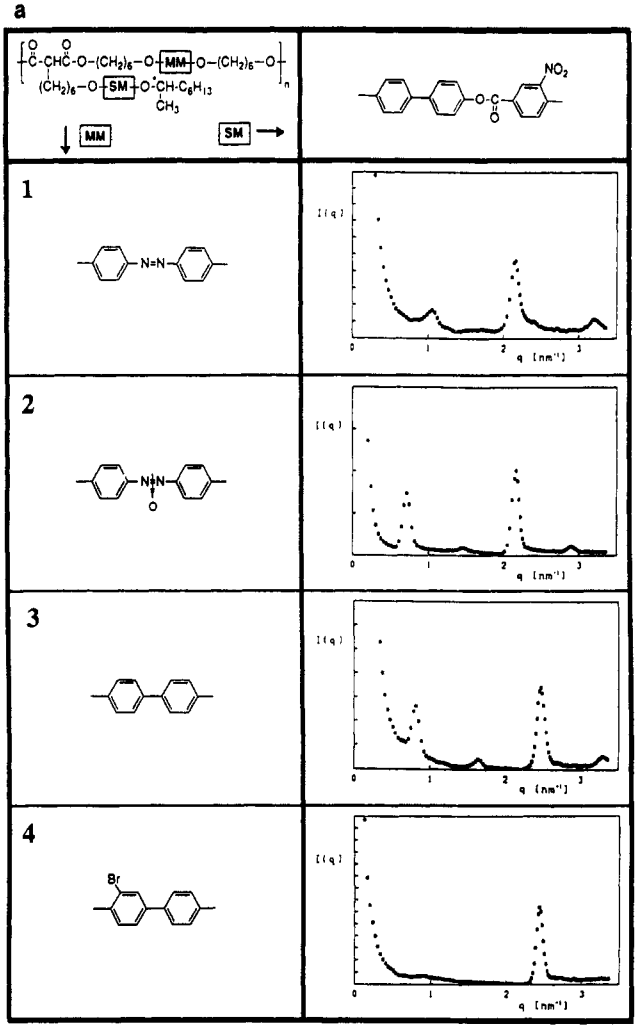

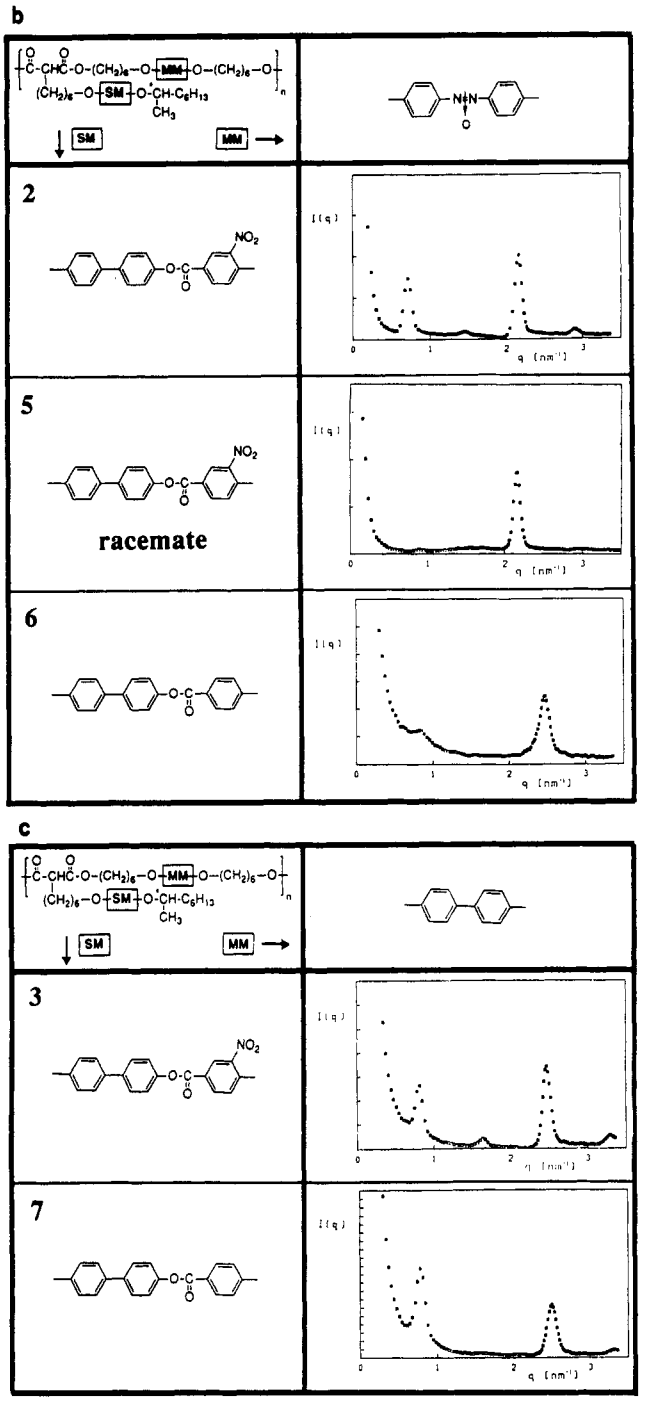

Figure 2. Room-temperature SAXS data from unoriented samples of (a) polymers **1–4** having the same chiral side-chain mesogen (SM) but different main-chain mesogens (MM) and of (b) polymers **2**, **5**, and **6** and (c) polymers **3** and **7**, having the same main-chain mesogen but different side-chain mesogens.

The precursor polymer C was synthesized via a melt polycondensation of the substituted malonic acid diethyl ester B and the diol A. Polymer-analogous esterification of the polymeric alcohol C and the racemic ether of 3-nitro-4-hydroxybenzoic acid D was done with the help of *N,N'*-dicyclocarbodiimide (DCC) and 4-(dimethylamino)pyridine (DMAP) at 0 °C. Polymer **5** could be recovered in good yields (90%). NMR measurements indicated the reaction to be quantitative within the limits of accuracy.[22,23]

The phase transitions for all polymers were determined by combining the data from DSC and X-ray measurements.[22] SAXS experiments on unoriented samples were performed at room temperature using a Kratky camera equipped with a one-dimensional position-sensitive detector (M Braun) and Ni-filtered Cu Kα radiation from a Siemens generator. After correcting for absorption and subtraction of the background intensity, desmeared intensities were obtained by applying a slit-correction procedure to the experimental data. For variable-temperature measurements, samples were enclosed in a homemade oven which maintained temperatures to within ±0.1 K. The layer spacings calculated from the SAXS data from different samples of the same polymer were found to be within ±0.03 nm of each other.

Oriented fibers were drawn from a pool of the isotropic melt; there was no significant improvement in the order upon annealing in the smectic phase. SAXS measurements on fibers were performed at room temperature using a Nicolet two-dimensional detector with a Rigaku rotating-anode X-ray source (λ = 0.154 nm). A graphite monochromator and a set of collimators placed ahead of the sample holder resulted in a beam diameter of ≈1.0 mm with a divergence of ≈0.056°. Fibers were mounted vertically, normal to the X-ray beam and at a distance of 460 mm from the detector.

Results

Unoriented Samples. Previous studies on combined LCPs have indicated that the main-chain and side-chain mesogens are incorporated within the same smectic layer and align parallel to each other.[7] X-ray measurements of the layer spacings in a series of combined chiral LCPs, including **1–7**, have been reported to be in the range of 2–3 nm.[17,22]

SAXS scans from unoriented samples of polymers **1–4**, measured at room temperature, are shown in Figure 2a.

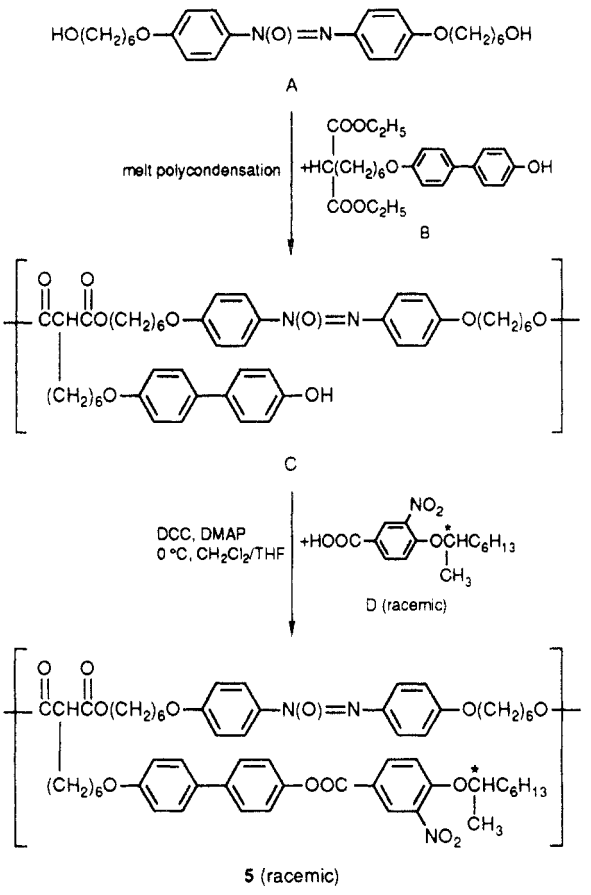

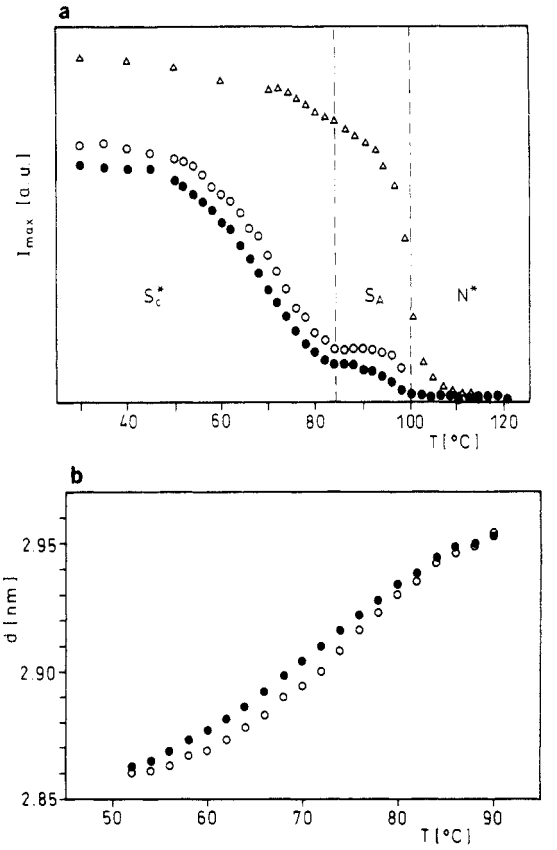

Figure 3. Temperature dependence of (a) intensities of the first-order (superstructure: heating, ○; cooling, ●) and third-order (smectic layer, △) peaks and (b) the layer spacing (heating, ○; cooling, ●) measured from the SAXS data of polymer 2.

It might be noted that polymers 1–4 have different main-chain mesogenic groups but the same chiral side-chain mesogenic group and exist in the frozen smectic-C* state at room temperature.[22] The SAXS data from polymer 1, for q ($=(4\pi \sin\theta)/\lambda$) less than 3.5 nm^{-1}, contain three peaks corresponding to 3 orders of the repeat distance of 5.80 nm. On the basis of previous X-ray studies,[22] it can be concluded that the strong second-order peak at 2.90 nm corresponds to the smectic layer spacing, implying that the first-order peak corresponding to the structural repeat originates from a bilayered superstructure. Variable-temperature mesurements on the positions of the first- and second-order peaks indicate a negligible temperature dependence in the S_{C^*} phase and a rapid loss of intensity at the S_{C^*}–N* (cholesteric) transition.

The SAXS scan from polymer 2 exhibits a strong peak corresponding to a d-spacing of 2.86 nm, which is comparable to the smectic layer spacing of 2.90 nm in 1. It is reasonable to assign this peak also to the smectic layer spacing, since the chemical structures of polymers 1 and 2 are very similar, except for the central azo and azoxy groups linking the phenyl rings in the respective main-chain mesogens. However, unlike the bilayered superstructure of 1, polymer 2 exhibits a superstructure corresponding to three layers, as indicated by the well-defined first- and second-order peaks at lower angles having d-spacings of ≈8.6 and 4.3 nm. The temperature dependence of the intensities of the first-order (superstructure) peak and the third-order (smectic layer) peak is shown in Figure 3a, and the variation in the position of the third-order peak with temperature is shown in Figure 3b. Polymer 2 has been characterized earlier as exhibiting the phase sequence S_{C^*}–S_A–N*–I.[22] In the temperature-dependent SAXS data, the continuous increase of the layer spacing, going from the S_{C^*} phase to the S_A phase, indicates that the S_{C^*}–S_A transition has second-order character. On the basis of the value of 2.96 nm for the S_A layer spacing, an apparent tilt angle of ≈15° can be calculated for the mesogens in the S_{C^*} phase. It is also interesting to note that the superstructure peak loses intensity more rapidly than the third-order smectic layer peak while approaching the S_A phase but still persists in the S_A phase. It disappears at the S_A–N* transition, along with the smectic layer peak, during the heating cycle and reappears upon cooling from the cholesteric phase. However, when the polymer is heated well into the isotropic phase (e.g., to 145 °C, which is 20 °C beyond the N*–I transition) and subsequently cooled, the superstructure peak appears only after the S_A–S_{C^*} transition. This indicates that the memory of the molecular organization within the superstructure is retained even in the cholesteric phase but can be obliterated by heating into the isotropic phase.

Trilayered superstructures are also exhibited by polymers 3 and 4, as evidenced by the corresponding SAXS data in Figure 2a. The strong third-order peaks, corresponding to the smectic layer spacings, have d-spacings of 2.52 and 2.59 nm in 3 and 4, respectively. These layer spacings are ≈0.3 nm smaller than those of 1 and 2. Going from the S_{C^*} to the S_A phase, the layer spacings increase slightly to 2.54 and 2.61 nm, respectively, from which an apparent tilt angle of ≈7° in the S_{C^*} phase can be calculated. This tilt angle is a factor of 2 smaller than the 15° tilt angle calculated for 2. Possible reasons for this will be discussed in the next section.

In an effort to explore possible correlations between the chemical structure and the formation of the trilayered superstructure, polymers 5–7, having slightly modified side-chain structures, were studied. Figure 2b compares the SAXS data from polymers 2, 5, and 6, measured at room temperature. Polymer 5 corresponds to a racemate of 2, with randomly substituted enantiomers of the side chain, while 6 has the same main-chain and side-chain

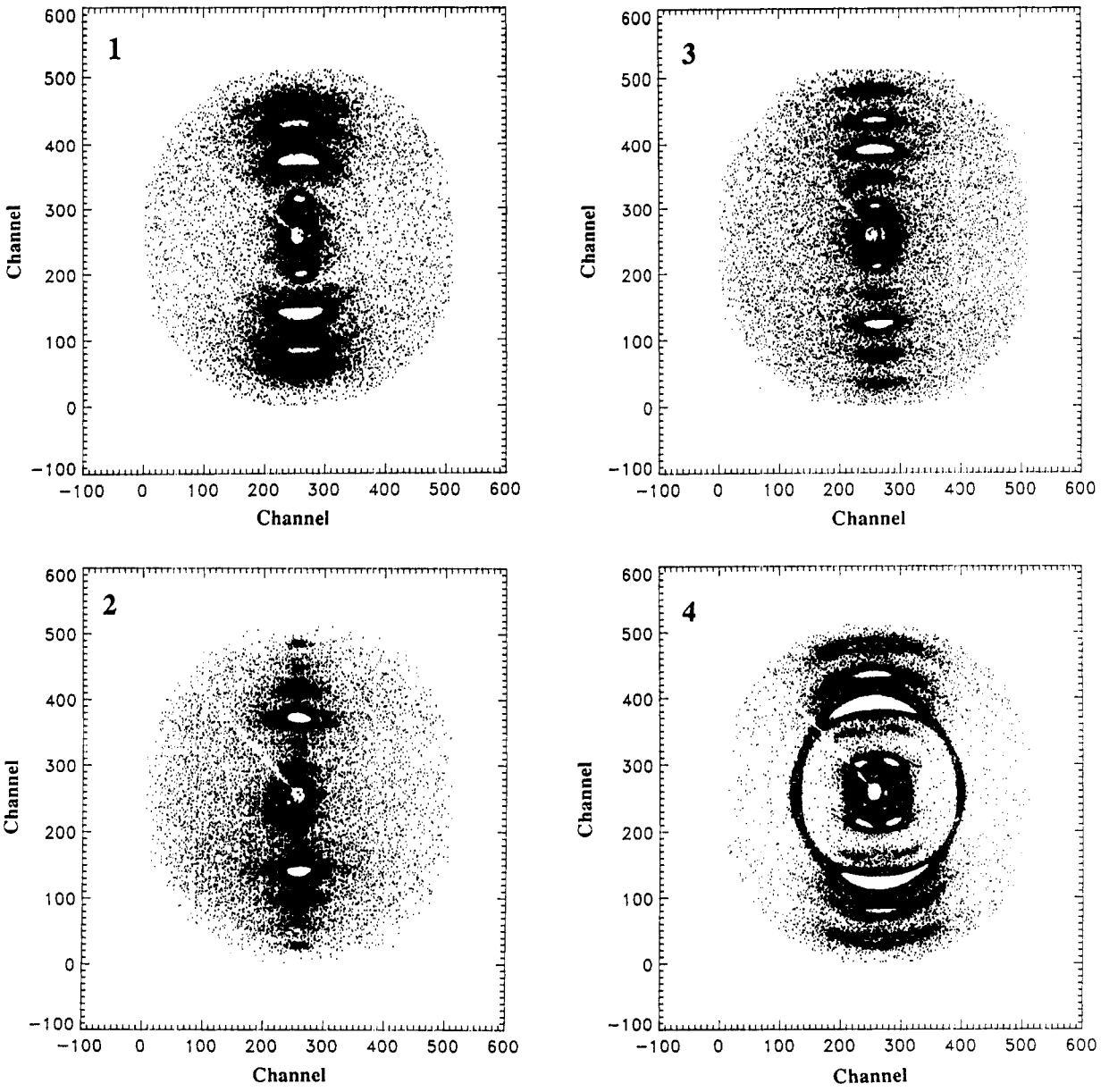

Figure 4. SAXS data from oriented fibers of polymers 1–4 recorded on an area detector. The fiber axis is vertical.

mesogens as **2**, except for the NO_2 side-chain substituent. The *d*-spacing of 2.89 nm for the peak in the SAXS data of **5**, corresponding to the smectic layer spacing, is similar to that of **2**. However, no superstructure peaks at lower angles can be resolved! This indicates that the enantiomeric purity of the side chains plays an important role in the formation of the superstructure. In the SAXS data of **6**, peaks corresponding to the trilayered superstructure can be observed although they are not as well-defined as in **2**. One can therefore conclude that the NO_2 substituent is not crucial to the formation of the superstructure. On the other hand, its effect on the smectic layer spacing appears to be significant since the 2.56-nm *d*-spacing of the third-order peak is 0.3 nm shorter than that of **2**. Furthermore, the apparent tilt angle of ≈23° in the S_{C^*} phase of **6**, based on the measurement of a 2.79-nm layer spacing in the S_A phase, is larger than the apparent tilt angle in **2**.

Figure 2c compares the SAXS data from polymers **3** and **7** whose chemical structures are identical except for the absence of the NO_2 side-chain substituent in the latter. The presence of a well-defined first-order peak corresponding to a trilayered superstructure in **7** again implies that the development of the supertructure is not dependent on the polar NO_2 substituent, similar to the observation in **6**. However, unlike **6**, the absence of the lateral substituent has a minimal effect on the layer spacing and apparent tilt angles, which were measured to be 2.51 nm and ≈5°, respectively.

Oriented Samples. Two-dimensional SAXS data from oriented fibers of polymers 1–4 are shown in Figure 4, with the fiber axes oriented vertically. In general, most of the peaks lie on the meridian (00*l* reflections), indicating that the smectic layer planes are normal to the fiber axis. The narrow angular distribution of peak intensities also points to the high degree of orientation in the fibers. The positions of the SAXS peaks are comparable to those observed in the unoriented data discussed above. There are, however, a few distinct features in the two-dimensional oriented data which are not distinguishable in the unoriented data. For example, besides the three well-defined peaks corresponding to orders of the bilayered superstructure in **1**, diffuse meridional peaks at $d \approx 3.5$ and 1.6 nm can also be observed. These diffuse peaks are incommensurate with respect to the bilayer spacing of 5.8 nm. They also do not correspond to satellites to the Bragg peaks, as have been observed, for example, in the diffraction data of some polar S_A liquid crystals.[25] It is likely that these aperiodic diffuse maxima are the result of transient defect structures which lead to additional density

modulations along the layer normal since their positions and relative intensities were found to be dependent on the thermal history of the sample.

The SAXS data from the fiber of polymer 4 are also different in that the first- and second-order superstructure peaks lie *off* the meridian while the strong third-order smectic layer peak lies *on* the meridian. (The arcing of the third-order peak in Figure 4 is an artifact arising as a result of selecting a low-intensity cutoff for plotting purposes.) The lateral shift of the first-order superstructure peak from the meridian corresponds to ≈ 0.48 nm^{-1} while the second-order peak is approximately twice as far from the meridian. These off-meridional peaks originate from structural modifications in a direction parallel to the smectic layers, as well be discussed later in greater detail. A low-intensity, highly arced equatorial maximum at $d \approx 2.6$ nm can also be observed in the fiber pattern. However, further heat treatment of the fiber in the smectic phase reduced its intensity below the background level.

Discussion

The SAXS data discussed above clearly indicate the presence of superstructures in the combined LCPs under study. Before discussing specific details of the superstructure in each individual polymer, a few general comments are worth mentioning. It has always been informative to compare the structure and properties of low molecular weight liquid crystals (LMLCs) with those of analogous polymeric liquid crystals. The topic of interest in the context of the present study is the formation of the S_{C^*} phase. There have been a number of theoretical and experimental investigations on the structure–property relationships in the S_{C^*} phase of LMLCs.[26] The presence of a chiral group is an obvious requirement. Its position relative to the rigid core and to polar groups in the molecule and the relative ease of rotation about the long axis of the molecule were found to significantly influence the stability of the S_{C^*} phase. Amongst the various intermolecular interactions, dipolar and quadrupolar interactions were found to be particularly important.[27] All the above factors determined the value and sign of the observed net polarization. In the combined LCPs under study, it is evident that the observed S_{C^*} phase and the presence of superstructures are intimately linked to the structure of the chiral side-chain mesogen. Structurally similar LMLCs containing an ester-linked biphenyl and phenyl moiety, with terminal alkyl or alkoxy chains containing at least an asymmetric carbon on one side, are known to exhibit S_{C^*} phases.[28] Detailed calorimetric, conoscopic, and electrooptical studies on the S_{C^*} phase of the liquid crystal MHPOBC, for example, have revealed the presence of not only a ferroelectric phase but also antiferroelectric and ferrielectric phases.[15] These phases are the result of local variations in the structural organization between layers, which imply the presence of superstructures. Studies performed on mixtures of chiral and achiral LMLCs are also relevant to the present investigations of combined LCPs. In general, such mixtures were found to be ferroelectric and the primary role of the achiral mesogens was that of an oriented matrix assisting in the ordering of the chiral mesogens.[29] It is, however, likely that, in combined LCPs, the polymeric character and the connectivity between the main chain and the side chains would affect the phase behavior and alter the nature/extent of interaction between mesogens. With this in mind, let us consider the relationship between the chemical structure and the characteristics of each polymer individually.

Polymer 1 exhibits a bilayered superstructure and a smectic layer spacing of 2.90 nm. In the analogous polymer without the side-chain mesogen, a smectic-A phase with a layer spacing of 3.60 nm has been reported.[30] It can therefore be concluded that the chiral side-chain mesogen induces the tilted S_{C^*} phase. As stated earlier, the S_{C^*} phase in 1 is followed directly by the cholesteric (N*) phase, as temperature increases, without an intermediate S_A phase. A similar phase sequence in chiral LMLCs has been attributed to significant interactions between layers.[26] Let us consider the influence of the structure of the polymer on the nature of interaction between layers. The NO_2 group is known to have a strong dipole moment (4.2 D).[31] Its lateral placement and the asymmetry of packing due to the presence of a chiral group in the side-chain mesogen should result in the formation of a net polarization within each smectic layer. The main-chain mesogen is not likely to contribute significantly to the polar interactions within the layer since it does not contain strongly polar groups. However, on the basis of the analogy with mixtures of achiral and chiral mesogens, it should be effective in ordering the chiral side-chain mesogens and thus enhance the net lateral polarization. Since it has been predicted that the presence of strong dipoles enhances the stability of antiferroelectric ordering over ferroelectric ordering,[26,32] it is very likely that the bilayered superstructure in 1 corresponds to an antiferroelectric ordering between the smectic layers, as shown schematically in Figure 5a. Indeed, recent studies on a side-chain LCP with a flexible polyacrylate backbone containing the same chiral mesogen, except for a slightly longer connecting flexible spacer, have indicated anomalous current and electrooptic responses, typical of antiferroelectric ordering.[33] SAXS studies have confirmed the presence of a bilayered superstructure in the side-chain LCP and the direct transformation of the S_{C^*} phase into the isotropic phase.[34]

The replacement of the central azo group in the main chain of 1 by an azoxy group in 2 leads to a trilayered superstructure in the latter, although the smectic layer spacings of both polymers are comparable. Also noteworthy is the fact that, in 2, an intermediate S_A phase exists between the S_{C^*} phase and the cholesteric phase. Therefore, it seems that the presence of the polar azoxy group in the main-chain mesogen alters the nature of interaction between mesogens within the layer and hence between layers. It is possible that the trilayered superstructure corresponds to a short helical pitch consisting of three smectic layers, each of which is rotated around the layer normal by 120°. In an effort to explore such a possibility, a thin film of 2 ($\approx$170 nm thick) was spin coated onto aluminum foil supported on a glass substrate. After annealing the film in the S_{C^*} phase for a few hours, an X-ray reflectivity measurement was performed. The reflectivity data clearly indicated the presence of the trilayered superstructure, with the smectic layers aligned parallel to the film surface. The positions of the SAXS peaks were in agreement with those from the bulk sample, indicating a negligible influence of the substrate on the organization in the thin film. Subsequently, the substrate was removed, and an X-ray transmission experiment, using an area detector, was performed on the coated foil with the incident beam normal to the film surface. Ideally, one should observe a six-point pattern in the wide-angle region corresponding to intermolecular distances between tilted mesogens in a helical superstructure comprising three ordered smectic layers. However, the data indicated only two arced reflections ($d \approx 0.45$ nm), which is inconsistent with a helical arrangement. Interestingly, dielectric relaxation measurements on polymer 2 have revealed a Goldstone mode characteristic of a ferroelectric phase,[35]

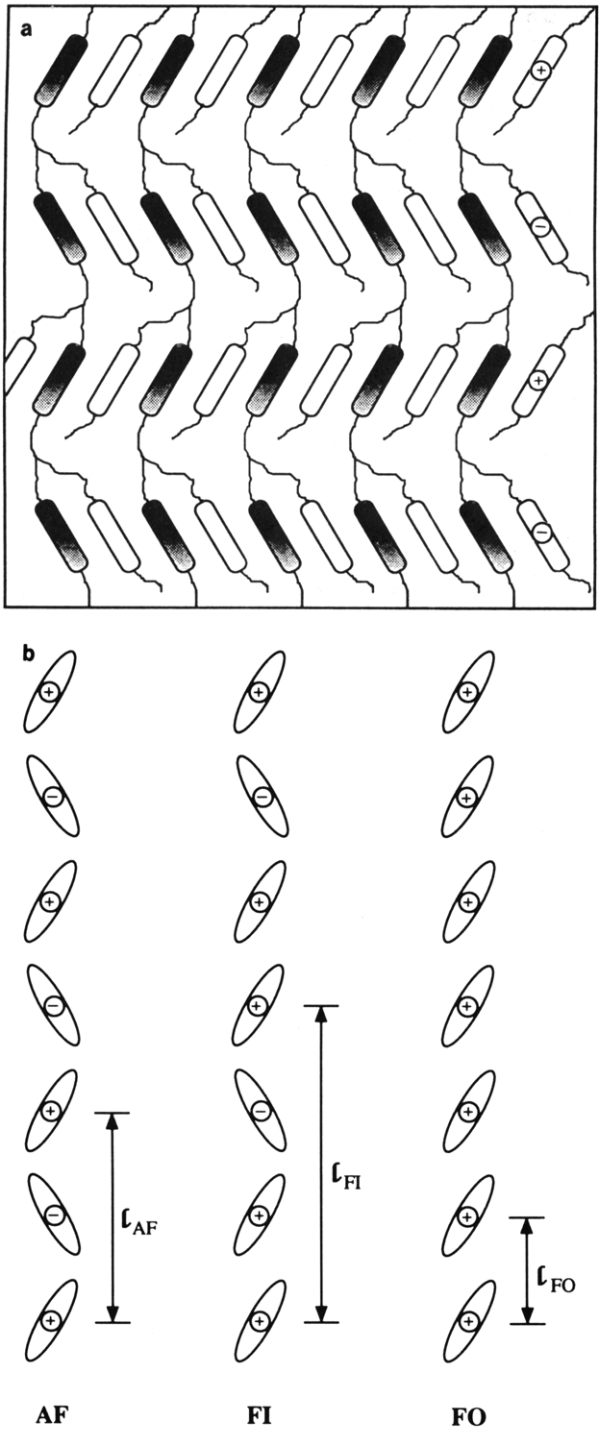

Figure 5. (a) Schematic model of antiferroelectric ordering in polymer **1**. The shaded and unshaded entities correspond to the main-chain and side-chain mesogens, respectively. (b) Schematic arrangement in the smectic layers corresponding to antiferroelectric (AF), ferrielectric (FI), and ferroelectric (FO) order. The structural repeat length in each of the arrangements is indicated. The + and − signs correspond to the direction of the net polarization going into and coming out of the plane of the figure, respectively.

which also rules out a local 3_1 helix. Since a purely ferroelectric phase would not exhibit a local superstructure, the trilayered superstructure is likely to correspond to a phase intermediate between ferroelectric ordering and antiferroelectric ordering. A possible model of the resulting *ferrielectric* ordering is shown schematically in Figure 5b. To our knowledge, such a phase has not been reported before in a polymeric liquid crystal! However, as mentioned earlier, a ferrielectric S_{C^*} phase has been observed in the low molecular weight liquid crystal MHPOBC, located in between the antiferroelectric S_{C^*} phase and the S_A phase. Out of the various structural models proposed for the ferrielectric phase, the model shown in Figure 5b was found to be the most consistent with respect to the analysis of the electrooptical and conoscopic data.[15] Comparison of the SAXS data from polymers **2**, **5**, and **6** sheds further light on the nature of the interaction between mesogens and the formation of the trilayered superstructure. In **5**, the presence of both R and S enantiomers of the side chain increases the symmetry within each smectic layer, resulting in no net polarization within the layer. Consequently, no superstructure is observed in the SAXS data. On the other hand, the presence of superstructure peaks in **6** indicates that, even in the absence of the strong lateral dipole from the NO_2 substituent, the contribution from the ester dipole in the side chain is sufficient to induce the formation of the superstructure. However, the absence of the lateral NO_2 substituent appears to affect the interaction between the main-chain and side-chain mesogens. In the S_A phase, a layer spacing of 2.96 nm in **2** compared to 2.79 nm in **6** indicates that the effective length of the combined mesogen is longer in **2**. The apparent tilt angles of the combined mesogens in the S_{C^*} phases of **2** and **6** are also different.

The chemical structure of polymer **3** corresponds to that of **1** or **2** without the central azo or azoxy functional group in the main-chain mesogen. However, the observed trilayered superstructure in **3** indicates a structural similarity with **2** rather than with **1**. Furthermore, temperature-dependent SAXS measurements also indicate the presence of a S_A phase in between the S_{C^*} and N* phases, similar to the phase behavior of **2**. As mentioned previously, the S_{C^*} layer spacing of 2.52 nm in **3** is ≈0.3 nm shorter in comparison to those of **1** and **2**. This difference is also maintained in the S_A phase and can be attributed to the influence of the structure of the main-chain mesogen. The biphenyl core of the main-chain mesogen in **3** is considerably shorter than corresponding core lengths in **1** and **2**. Therefore, the overlap between the main-chain and side-chain mesogens in **2** and **3** is likely to be different. This is clearly demonstrated by the fact that the layer spacings in **2** and **6** are significantly affected by the presence or absence of the side-chain NO_2 substituent but remain nearly constant in **3** and **7**. The relatively short length of the core is also likely to increase the contribution of the conformation of the flexible spacers to the overall layer separation. The small value of the apparent tilt angle (≈7°) in **3** may be related to this fact. In this context, calculation of the tilt angle based on the model of rigid rods may not be appropriate. In the rigid-rod model, the tilt angle is computed as $\theta = \cos^{-1}(d_C/d_A)$, where d_C and d_A are the layer spacings of the S_{C^*} and the S_A phases, respectively. The conformation of the flexible spacers attached to the rigid cores is not explicitly considered. In some LMLCs with aliphatic tails, it has been reported that the tilt angle of the rigid core determined by optical methods is always larger than the tilt angle determined by X-ray scattering.[36] This has led to the proposal of the "zigzag" model which includes the conformation of the flexible tails.[37] In **3**, the ratio of the length of the main-chain mesogenic core to the S_{C^*} layer spacing is small compared to the corresponding ratio in **2**. Therefore, a change in the tilt angle of the rigid core may not be reflected by a proportional change in the layer spacing due to independent conformational changes in the flexible spacers. The small value of the tilt angle in **3** in comparison to **2** may be the manifestation of such an effect.

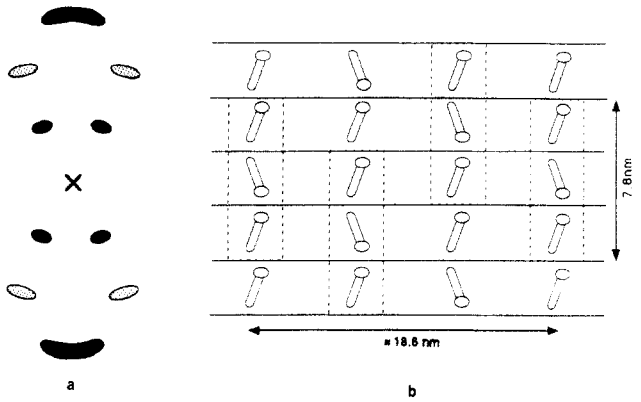

Figure 6. (a) Schematic representation of the relative positions and intensities of the first-, second-, and third-order peaks in the fiber pattern of polymer 4. (b) Possible model depicting structural modulations between and across the smectic layers in polymer 4. The presence of steric hindrance between mesogens in 4 is represented by the asymmetric shape of the repeating unit, and the dashed box encloses the trilayered structural repeat in the direction of the layer normal.

The introduction of Br as a lateral substituent leads to lower transition temperatures in polymer 4 in comparison to polymer 3.[22] The lowering of transition temperatures as a result of steric hindrance due to lateral substituents is well documented in the literature.[38] It is surprising that the layer spacings and apparent tilt angles in 3 and 4 are similar since the laterally substituted Br atom with its associated polarizability is likely to alter interparticle interactions within the layer. The splitting of the first- and second-order peaks observed in the fiber pattern of 4 in Figure 4 is a likely result of such interactions. Figure 6a schematically shows the relative positions and intensities of the first-, second-, and third-order peaks. Such a pattern is inconsistent with a simple tilt of the smectic planes with respect to the fiber axis. It can be explained by the presence of structural modulations in the direction parallel to the smectic layers. Similar observations of transverse structural modulations in S_A and S_C phases in LMLCs have been reported in the literature.[39] A theoretical interpretation by Prost describes such modulations to be the result of a two-dimensional escape from incommensurability.[40] In the case of 4, incommensurability probably arises due to the different lengths and/or directions of the wave vectors corresponding to planes of equal dipolar density and mass density. A possible model for the structural organization along and normal to the smectic planes, consistent with the fiber pattern of 4, is shown in Figure 6b. The trilayered repeat unit undergoes a modulation in the direction of the smectic layer with a period of approximately 18.6 nm, based on the lateral shift of the first-order peak in the fiber pattern.

The present SAXS study of combined chiral LCPs represents the first observation of bilayered and trilayered superstructures for which we have proposed antiferroelectric and ferrielectric ordering, respectively. It is obvious that further studies using other characterization methods, especially electrooptical measurements, are necessary for a better and complete understanding of these complex systems. However, the high viscosities of the combined LCPs are a hindrance toward the formation of monodomains, which are essential for an unambiguous characterization of the phase and structure. Currently, work on a more detailed understanding of the structure–property relationships in the chiral side-chain mesogen alone is also in progress and will be reported in the near future.

Conclusions

SAXS studies on a series of combined liquid crystal polymers containing achiral main-chain mesogens and chiral side-chain mesogens reveal the presence of novel superstructures which have not been observed previously in similar polymers. On the basis of the analysis of SAXS data from unoriented and oriented samples and structural models in similar low molecular weight liquid crystals, the bilayered superstructure is attributed to antiferroelectric ordering while ferrielectric ordering is proposed for the trilayered superstructures. The chemical structures of the main-chain and side-chain mesogens and the interactions between them determine the smectic layer spacing and influence the formation of the superstructure. The presence of unichirality and polar groups which lead to a net polarization within the smectic layer are considered to be primary factors controlling the formation of superstructures. In the polymers under study, changing the structure of the achiral main-chain mesogen affects the smectic layer spacing. Furthermore, the presence of bulky laterally substituted side groups leads to structural modulations within the smectic layers while maintaining the superstructure normal to the layers. While the SAXS studies reveal a lot of information about the structure and phase behavior of the combined chiral LCPs, further studies using other characterization methods are required for a better understanding of these complex systems.

Acknowledgment. We thank Prof. E. W. Fischer, Dr. M. Stamm, Dr. C. Boeffel, Priv. Doz. Dr. R. Zentel, and Dr. H. Freimuth for helpful discussions.

References and Notes

(1) McArdle, C. B., Ed. *Side Chain Liquid Crystal Polymers*; Blackie and Son Ltd.: Glasgow, Scotland, 1989.
(2) Blumstein, A. *Liquid Crystalline Order in Polymers*; Plenum Press: New York, 1985.
(3) Weiss, R. A.; Ober, C. K., Eds. *Liquid Crystal Polymers*; ACS Symposium Series 435; American Chemical Society: Washington, DC, 1990.
(4) Engel, M.; Hisgen, B.; Keller, R.; Kreuder, W.; Reck, B.; Ringsdorf, H.; Schmidt, H.-W.; Tschirner, P. *Pure Appl. Chem.* **1985**, *57*, 1009.
(5) Zentel, R.; Schmidt, G. F.; Meyer, J.; Benalia, M. *Liq. Cryst.* **1987**, *2*, 651.
(6) Reck, B.; Ringsdorf, H. *Makromol. Chem., Rapid Commun.* **1985**, *6*, 291.
(7) Reck, B.; Ringsdorf, H. *Makromol. Chem., Rapid Commun.* **1986**, *7*, 389.
(8) See for example: Gray, G. W.; Goodby, J. W. G. *Smectic Liquid Crystals*; Leonard Hill: Glasgow and London, 1984. Pershan, P. S. *Structure of Liquid Crystal Phases*; World Scientific Lecture Notes in Physics, World Scientific: London, 1988; Vol. 23.
(9) Levelut, A. M. *J. Phys., Lett.* **1984**, *45*, L603.
(10) Sigaud, G.; Hardouin, F.; Achard, M. F.; Gasparoux, H. *J. Phys., Colloq.* **1979**, *40*, C3-356. Sigaud, G.; Hardouin, F.; Achard, M. F. *Phys. Lett.* **1979**, *72A*, 24.
(11) Meyer, R. B.; Liebert, L.; Strzelecki, L.; Keller, P. *J. Phys., Lett.* **1975**, *36*, L69.
(12) See for example: Bahadur, B., Ed. *Liquid Crystals: Applications and Uses*; World Scientific: Singapore, 1990; Vol. 1.
(13) Gorecka, E.; Chandani, A. D. L.; Ouchi, Y.; Takezoe, H.; Fukuda, A. *Jpn. J. Appl. Phys.* **1990**, *29*, 131.
(14) Chandani, A. D. L.; Ouchi, Y.; Takezoe, H.; Fukuda, A.; Terashima, K.; Furakawa, K.; Kishi, A. *Jpn. J. Appl. Phys.* **1989**, *28*, L1261.
(15) Takezoe, H.; Lee, J.; Ouchi, Y.; Fukuda, A. *Mol. Cryst. Liq. Cryst.* **1991**, *202*, 85.
(16) See for example: Le Barny, P.; Dubois, J. C. In *Side Chain Liquid Crystal Polymers*; McArdle, C. B., Ed.; Blackie and Son Ltd.: Glasgow, Scotland, 1989; p 130.
(17) Kapitza, H.; Zentel, R. *Makromol. Chem.* **1988**, *189*, 1793.
(18) Meier, W.; Finkelmann, H. *Makromol. Chem., Rapid Commun.* **1990**, *11*, 599.

(19) Vallerien, S. U.; Kremer, F.; Fischer, E. W.; Kapitza, H.; Zentel, R.; Poths, H. *Makromol. Chem., Rapid Commun.* **1990**, *11*, 593.
(20) Ushida, S.; Morita, K.; Myoshi, K.; Hashimoto, K.; Kawasaki, K. *Mol. Cryst. Liq. Cryst.* **1988**, *155*, 95.
(21) Scherowsky, G.; Kühnpast, K.; Springer, J. *Makromol. Chem., Rapid Commun.* **1991**, *12*, 381.
(22) Kapitza, H.; Zentel, R. *Makromol. Chem.* **1991**, *192*, 1859.
(23) Poths, H.; Zentel, R.; Vallerien, S. U.; Kremer, F. *Mol. Cryst. Liq. Cryst.* **1991**, *203*, 101.
(24) Kapitza, H.; Zentel, R.; Twieg, R. J.; Nguyen, C.; Vallerien, S. U.; Kremer, F.; Wilson, C. G. *Adv. Mater.* **1990**, *2*, 539.
(25) Levelut, A. M. In *Incommensurate Crystals, Liquid Crystals and Quasi-crystals*; Scott, J. F., Clark, N. A., Eds.; Plenum Press: New York and London, 1987; p 283.
(26) Goodby, J. W.; Leslie, T. M. *Mol. Cryst. Liq. Cryst.* **1984**, *110*, 175. Inukai, I.; Saitoh, S.; Inoue, M.; Miyazawa, K.; Furukawa, K. *Mol. Cryst. Liq. Cryst.* **1986**, *141*, 237. Beresnev, L. A.; Blinov, L. M.; Osipov, M. A.; Pikin, S. A. *Mol. Cryst. Liq. Cryst.* **1988**, *158A*, 1.
(27) Urbanc, B.; Zeks, B. *Liq. Cryst.* **1989**, *5*, 1075 and references therein.
(28) Terashima, K.; Ichihashi, M.; Kikuchi, M.; Furukawa, K.; Inukai, I. *Mol. Cryst. Liq. Cryst.* **1986**, *141*, 237.
(29) Buka, A.; Stegemeyer, H. *Liq. Cryst.* **1990**, *8*, 229 and references therein.
(30) Voigt-Martin, I. G.; Durst, H.; Reck, B.; Ringsdorf, H. *Macromolecules* **1988**, *21*, 1620.
(31) Staab, H. A. *Einführung in die Theoretische Organische Chemie*; Verlag Chemie: Darmstadt, Germany, 1975.
(32) Longa, L.; de Jeu, W. H. *Phys. Rev. A* **1983**, *28*, 2380.
(33) Skarp, K.; Andersson, G.; Lagerwall, S. T.; Kapitza, H.; Poths, H.; Zentel, R. *Ferroelectrics*, in press.
(34) Mensinger, H.; Poths, H.; Skarp, K.; Zentel, R., work in progress.
(35) Vallerien, S. U. Ph.D. Thesis, University of Mainz, 1990.
(36) Ostrovskii, B. I. X-ray Diffraction Study of Nematic, Smectic A and C Liquid Crystals. *Sov. Sci. Rev.: Phys. Rev.* **1989**, *12*.
(37) Bartolino, E.; Doucet, J.; Durand, G. *Ann. Phys. (Paris)* **1978**, *3*, 389.
(38) Gray, G. W., Winsor, P. A., Eds. *Liquid Crystals and Plastic Crystals*, Harwood: Chichester, U.K., 1974.
(39) Levelut, A. M.; Tarento, R. J.; Hardouin, F.; Archard, M. F.; Sigaud, G. *Phys. Rev. A* **1981**, *24*, 163. Huang, C. C.; Lien, S. C.; Dumrongrattana, S.; Chiang, L. Y. *Phys. Rev. A* **1984**, *30*, 965.
(40) Prost, J. *Adv. Phys.* **1984**, *33*, 1.

Registry No. 1 (copolymer) ester, 141017-09-6; 2 (copolymer) ester, 141062-03-5; 3 (copolymer) ester, 141017-10-9; 4 (copolymer) ester, 141017-11-0.